L.I. Anatychuk[1,2], R.R. Kobylianskyi[1,2]

L.I. Anatychuk

[1]Institute of Thermoelectricity of the NAS and MES Ukraine, 1, Nauky Str., Chernivtsi, 58029, Ukraine;
[2]Yu. Fedkovych Chernivtsi National University, 2, Kotsyubinsky Str., Chernivtsi, 58000, Ukraine

R.R. Kobylianskyi

SOME SPECIFIC FEATURES OF DYNAMIC OPERATING MODES OF THERMAL GENERATOR USING HUMAN HEAT

The paper deals with the advisability of using dynamic operating modes of thermoelectric microgenerators for power supply to low-power equipment. The effect of connecting plate geometry and thermal generator dimensions on their energy characteristics is investigated. It is established that dynamic operating modes of short-life thermoelectric power sources are more expedient, since under certain conditions they afford an opportunity to produce twice as high electric power compared to steady-state modes.

Key words: thermoelectric microgenerator, dynamic mode, human heat release, computer simulation.

Introduction

Using human heat for power supply to various low-power electronic devices with the aid of thermoelectric microgenerators generates growing interest [1-6]. There are wrist watches with a thermoelectric power source [7-13], wireless autonomous pulse meters [3, 14], electronic medical thermometers [15-18], wrist oxymeters [19], wireless electroencephalographs [20-22], thermoelectric microgenerators for mounting into clothes [23-26], etc. They can be short-life, such as electronic medical thermometer with a thermoelectric power source measuring human body temperature within several minutes. Indeed, with such devices one does not need much time to get information on human temperature. And the sooner this information is obtained, the more efficient is thermometer operation. Under these conditions, the use of steady-state operating modes may prove to be unjustified. Naturally, steady-state operating mode of a thermoelectric generator after it touches human body generally occurs in several minutes, and to measure human body temperature with electronic medical thermometer it is enough to have several tens of seconds. Therefore, in such cases a thermoelectric microgenerator should be used in transient operating modes that are dealt with in this paper.

1. A physical model of biological tissue with a thermoelectric microgenerator and a heat sink

According to a physical model (Fig. 1), an area of human skin is a structure consisting of three layers (epidermis 1, dermis 2, subcutis 3) and internal tissue 4. This structure is characterized by thermal conductivity κ_i, specific heat C_i, density ρ_i, blood perfusion rate ω_b, blood density ρ_b, blood heat capacity C_b and specific heat release q_{met} due to metabolic processes (Table 1). The respective biological tissue layers 1 – 4 are regarded as the bulk sources of heat q_i, where:

$$q_i = q_{meti} + \rho_b \cdot C_b \cdot \omega_{bi} \cdot (T_b - T), \quad i = 1..4. \tag{1}$$

The geometric dimensions of each such layer are a_i, b_i and l_i. The temperatures at the boundaries of the respective biological tissue layers are T_1, T_2, T_3 and T_4.

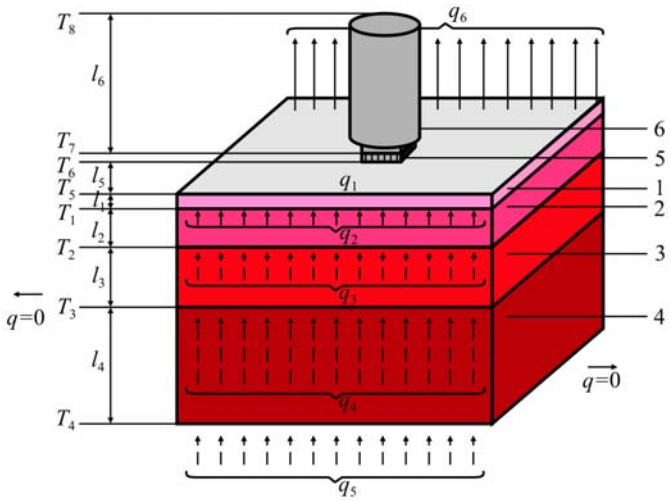

Fig. 1. A physical model of biological tissue with a thermoelectric microgenerator and a heat sink: 1 – epidermis, 2 – dermis, 3 – subcutis, 4 – internal tissue, 5 – thermoelectric microgenerator, 6 – heat sink.

A thermoelectric microgenerator 5 is a rectangular bar with dimensions a_5, b_5, l_5, characterized by thermal conductivity coefficient κ. The thermoelectromotive force of thermoelectric generator is known to be determined as [1, 2]:

$$E = \alpha \cdot N \cdot \Delta T, \tag{2}$$

where α is the Seebeck coefficient, N is the number of thermoelectric material legs, ΔT is temperature difference between the microgenerator's upper and lower surfaces. The number of thermoelectric material legs in the microgenerator is N = 1500 – 3000 pcs. Simulation of a thermogenerator with such a number of elements is an intricate problem even for modern personal computers.

Table 1

Thermophysical properties of human biological tissue [27-31]

Biological tissue layers	Epidermis	Dermis	Subcutis	Internal tissue
Thickness, l (mm)	0.08	2	10	30
Specific heat, S ($J \cdot kg^{-1} \cdot K^{-1}$)	3590	3300	2500	4000
Thermal conductivity, κ ($W \cdot m^{-1} \cdot K^{-1}$)	0.24	0.45	0.19	0.5
Density, ρ ($kg \cdot m^{-3}$)	1200	1200	1000	1000
Metabolism, q_{met} ($W \cdot m^{-3}$)	368.1	368.1	368.3	368.3
Tissue blood perfusion rate, ω_b ($m^3 \cdot s^{-1} \cdot m^{-3}$)	0	0.00125	0.00125	0.00125
Blood density, ρ_b ($kg \cdot m^{-3}$)	1060	1060	1060	1060
Blood heat capacity, C_b ($J \cdot kg^{-1} \cdot K^{-1}$)	3770	3770	3770	3770

At the same time, from formula (2) it is evident that the thermogenerator's EMF value is mainly influenced by temperature difference ΔT between its surfaces. Therefore, to reach the purpose set in this paper, it is quite sufficient to replace a thermoelectric microgenerator having a large number of elements by the bulk homogeneous sample of equivalent thermal conductivity κ. Then, on the basis of calculated ΔT, one can easily determine the microgenerator's EMF according to formula (2).

The thermoelectric microgenerator 5 with geometric dimensions a_5, b_5, l_5 and contact surface temperature T_6 is located on the surface of biological tissue (epidermis 1) with temperature T_5. The thermoelectric microgenerator 5 is in the state of heat exchange with heat sink 6 of high thermal conductivity material with geometric dimensions a_6, b_6, l_6 and contact surface temperature T_7.

Free surface of skin area (epidermis 1) is in the state of heat exchange with the environment with temperature T_8 which is taken into account by heat exchange coefficient α. The rest of free surfaces of thermoelectric micogenerator 5 and heat sink 6 are adiabatically isolated. The specific heat flux from the free skin surface is q_6, and the specific heat flux from the internal human bodies is q_5. Skin heat exchange due to radiation and perspiration is disregarded.

As long as a physical model is an area of a four-layered biological tissue, with identical biochemical processes occurring in adjacent layers, it can be assumed that there is no heat overflow through the lateral surface of biological tissue ($q = 0$).

2. Mathematical description of the model

As long as this research aims at studying the dynamics of physical processes in a thermoelectric microgenerator since the moment it is brought into thermal contact with the skin surface, one must know the steady-state distribution of temperature in biological tissue in the absence of microgenerator on its surface. Such temperature distribution should be chosen as the initial conditions in biological tissue in the process of thermal interaction between thermoelectric microgenerator and biological tissue. This, in turn, means that the research should be performed in two steps. At the first step it is necessary to find the steady-state temperature distribution in biological tissue in the absence of a microgenerator on its surface. At the second step – the dynamic temperature distribution in biological tissue and the thermoelectric microgenerator and heat sink located on its top, assuming as the initial conditions for biological tissue the temperature distribution found at the first step.

A general equation of heat exchange in biological tissue is as follows [27-31]:

$$\rho_i \cdot C_i \cdot \frac{\partial T}{\partial t} = \nabla(\kappa_i \cdot \nabla T) + \rho_b \cdot C_b \cdot \omega_{b_i} \cdot (T_b - T) + q_{met_i}, \tag{3}$$

where $i = 1...4$ are corresponding layers of biological tissue, ρ_i is the density of corresponding biological tissue layer (kg/m^3), C_i is specific heat of corresponding biological tissue layer (J/kg·K), ρ_b is blood density (kg/m^3), C_b is specific heat of blood (J/kg·K), ω_{bi} is blood perfusion rate of corresponding biological tissue layer (m^3·s^{-1}·m^{-3}), T_b is human blood temperature (°C), where $T_b = 37$ °C, q_{meti} is the amount of metabolic heat of corresponding biological tissue layer (W/m^3), T is absolute temperature (K), κ_i is thermal conductivity coefficient of corresponding biological tissue layer (W/m·K), t is time (s).

The summand in the left-hand side of equation (3) is the rate of change in thermal energy comprised in the unit volume of biological tissue. Three summands in the right-hand side of this equation are the rate of change in thermal energy due to thermal conductivity, blood perfusion and metabolic heat, respectively.

At the first step of research $\frac{\partial T}{\partial t} = 0$, so Eq.(3) is simplified as:

$$\nabla(\kappa_i \cdot \nabla T) + \rho_b \cdot C_b \cdot \omega_{b_i} \cdot (T_b - T) + q_{met_i} = 0. \tag{4}$$

Steady-state equation of heat exchange in biological tissue (4) is solved with the boundary conditions (5) yielding the distribution $T(x, y, z)$

$$\begin{cases} q\big|_{x=0} = 0, \\ q\big|_{x=a} = 0, \end{cases} \begin{cases} q\big|_{y=0} = 0, \\ q\big|_{y=a} = 0, \end{cases} \begin{cases} T\big|_{z=0} = 37\ ^\circ\mathrm{C}, \\ q\big|_{z=b} = \alpha \cdot (T_0 - T), \end{cases} \tag{5}$$

where q is heat flux density, T is absolute temperature, T_0 is ambient temperature, α is heat exchange coefficient.

At the second step, a dynamic temperature distribution in the biological tissue is found by solving Eq.(3) with the boundary conditions (5) and the initial temperature distribution $T(x, y, z)$. In so doing, in thermoelectric microgenerator and heat sink we solve a general equation of heat exchange [1, 2, 32]:

$$\rho_i \cdot C_i \cdot \frac{\partial T}{\partial t} = \nabla(\kappa_i \cdot \nabla T), \tag{6}$$

where $i = 5, 6$ is thermal generator and heat sink material, ρ_i is substance density, C_i is substance specific heat, κ_i is thermal conductivity coefficient. The boundary conditions for Eq.(6) include adiabatic insulation of surfaces of thermoelectric microgenerator and the initial temperature distribution $T = \text{const} = T_{amb.}$

3. Computer simulation

To study the dynamic operating modes of thermoelectric microgenerators using human heat, a three-dimensional computer model of biological tissue was created having on its top a thermoelectric microgenerator and a heat sink. The computer model was constructed with the aid of Comsol Multiphysics applied program package [33] allowing simulation of thermophysical processes in biological tissue with regard to blood circulation and metabolism.

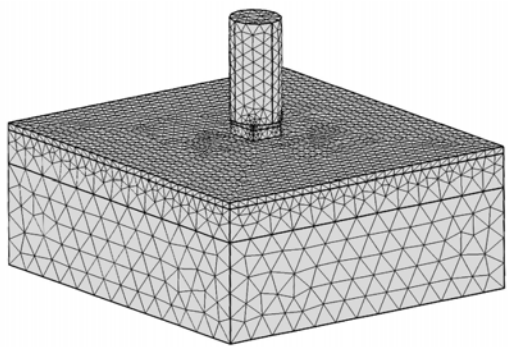

Fig. 2. Finite element method mesh.

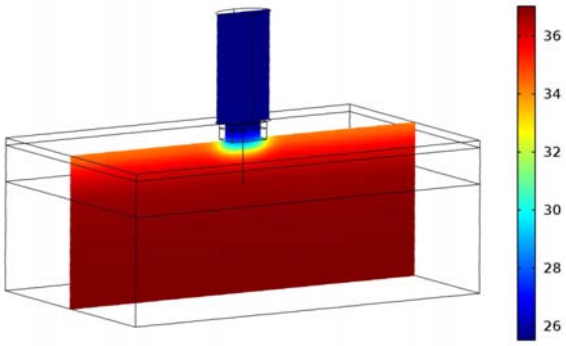

Fig. 3. Temperature distribution in the section of human biological tissue having on its top a thermoelectric microgenerator and heat sink.

The distribution of temperature and heat flux density in the biological tissue, thermoelectric microgenerator and heat sink was calculated by the finite element method (Fig. 2). According to this method, an object under study is split into a large number of finite elements, and in each of them the value of function is sought which satisfies given differential equations of second kind with the respective boundary conditions. The accuracy of solving the formulated problem depends on the level of splitting and is assured by using a large number of finite elements [33].

Object-oriented computer simulation was used to obtain the distributions of temperature (Fig. 3) and heat flux density lines in human biological tissue, thermoelectric microgenerator and heat sink.

4. Computer simulation results

Figs. 4, 5 represent a dynamics of change in EMF and electric power of thermoelectric microgenerators (with dimensions 10 × 10 mm, 15 × 15 mm, 20 × 20 mm) using human heat at ambient temperatures $T = (20 \div 36)$ °C with and without regard to blood circulation in biological tissue.

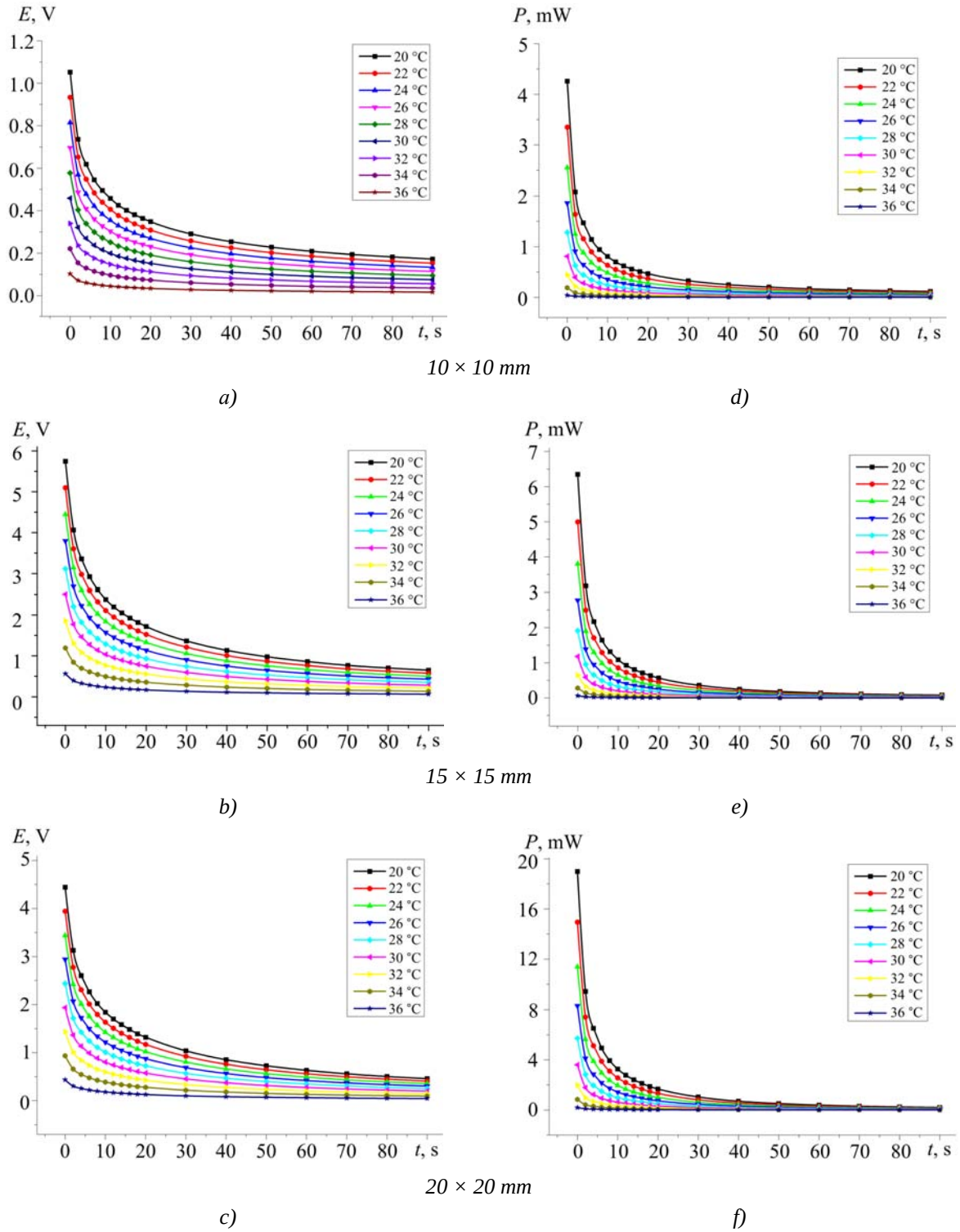

Fig. 4. Dynamics of change in EMF (a, b, c) and electric power (d, e, f) of thermoelectric microgenerator without regard to blood circulation in biological tissue: a), d) for microgenerator with dimensions 10 × 10 mm; b), e) for microgenerator with dimensions 15 × 15 mm; c), f) for microgenerator with dimensions 20 × 20 mm.

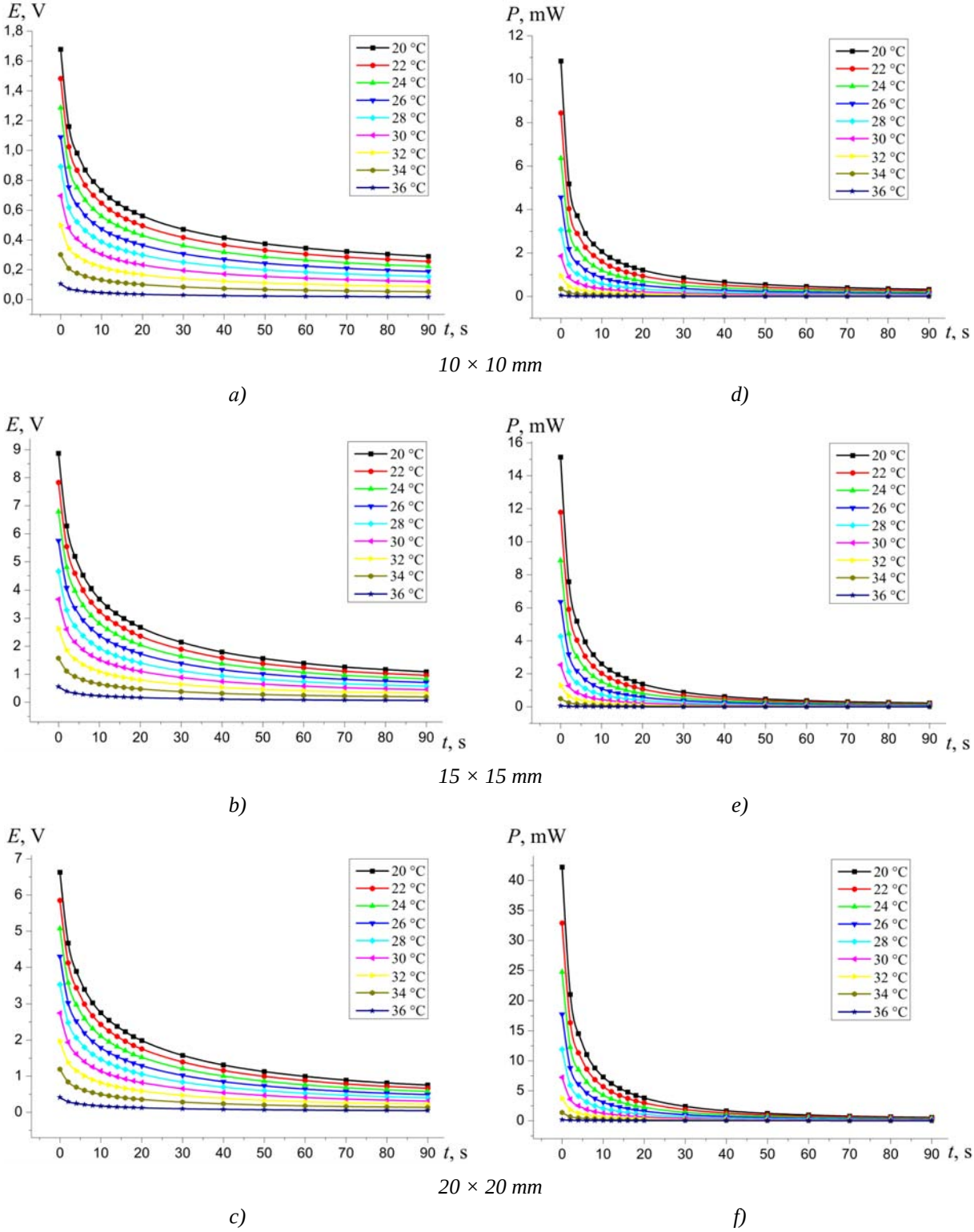

Fig. 5. Dynamics of change in EMF (a,b, c) and electric power (d, e, f) of thermoelectric microgenerator with regard to blood circulation in biological tissue: a), d) for microgenerator with dimensions 10 × 10 mm; b), e) for microgenerator with dimensions 15 × 15 mm; c), f) for microgenerator with dimensions 20 × 20 mm.

Analyzing Figs. 4, 5, we see that blood circulation in biological tisue affects considerably the energy charactertistics of thermoelectric microgenerators. Thus, for instance, for the case of a thermal generator with dimensions 10 × 10 mm the EMF differs by a factor of 1.6, and electric power P – by a

factor of 2.6; for the case of 15 × 15 mm the EMF differs by a factor of 1.55, and electric power P – by a factor of 2.4; and for the case of 20 × 20 mm the EMF differs by a factor of 1.5, and electric power P – by a factor of 2.2. Thus, with increasing dimensions of thermoelectric microgenerator, the influence of blood circuilation in biological tissue on its energy characteristics is reduced.

5. Experimental investigations

5.1. Experimental procedure

To perform experimental investigations of the dynamic modes of thermoelectric microgenerators, samples with dimensions 10 × 10 mm, 15 × 15 mm, 20 × 20 mm and their respective hollow copper heat sinks with pipes for pumping thermostated liquid through them were made. Characteristics of thermoelectric microgenerators are given in Table 2. For liquid thermostating a thermoelectric thermostat was used that allows keeping given liquid temperature to an accuracy of ± 0.1 °C. Thus, thermostated copper heat sinks imitate thermal effect of environment on thermoelectric microgenerator.

As a source of heat, the surface of human skin in armpit area was used (typical zone of human body temperature measurement).

Table 2

Characteristics of experimental samples of thermoelectric microgenerators

Characteristics of microgenerators	Sample 1	Sample 2	Sample 3
Microgenerator dimensions, mm	10 × 10	15 × 15	20 × 20
Number of legs, pcs	624	3440	2496
Electric resistance R, Ω	130	2600	520
Dimensions of legs, mm	0.35 × 0.35 × 3	0.2 × 0.2 × 3	0.35 × 0.35 × 3

Digital multimeter M3500A connected to a personal computer was used to register the dynamics of change in the EMF of thermoelectric microgenerators within 90 seconds since the moment of their application to skin surface. Based on the measured values of EMF E, full power P of thermoelectric microgenerators was calculated according to expression:

$$P = \frac{E^2}{2 \cdot R}. \tag{7}$$

5.2. Experimental results

Fig. 6 shows a dynamics of change in the EMF and electric power of experimental thermoelectric microgenerators at ambient temperatures T = (24 ÷ 34) °C.

As a result of analysis of Figs. 4, 5 a feature common to all calculated curves has been revealed that is not typical of the dynamic operating conditions of experimental thermoelectric microgenerators. It lies in the fact that the calculated values of microgenerator energy characteristics are maximum at the initial time instant when thermoelectric generator makes contact with skin surface.

However, in fact it is clear that characteristics of microgenerator under isothermal conditions are equal to zero, including the moment of contact to skin surface, which is confirmed by experimental data (Fig. 6).

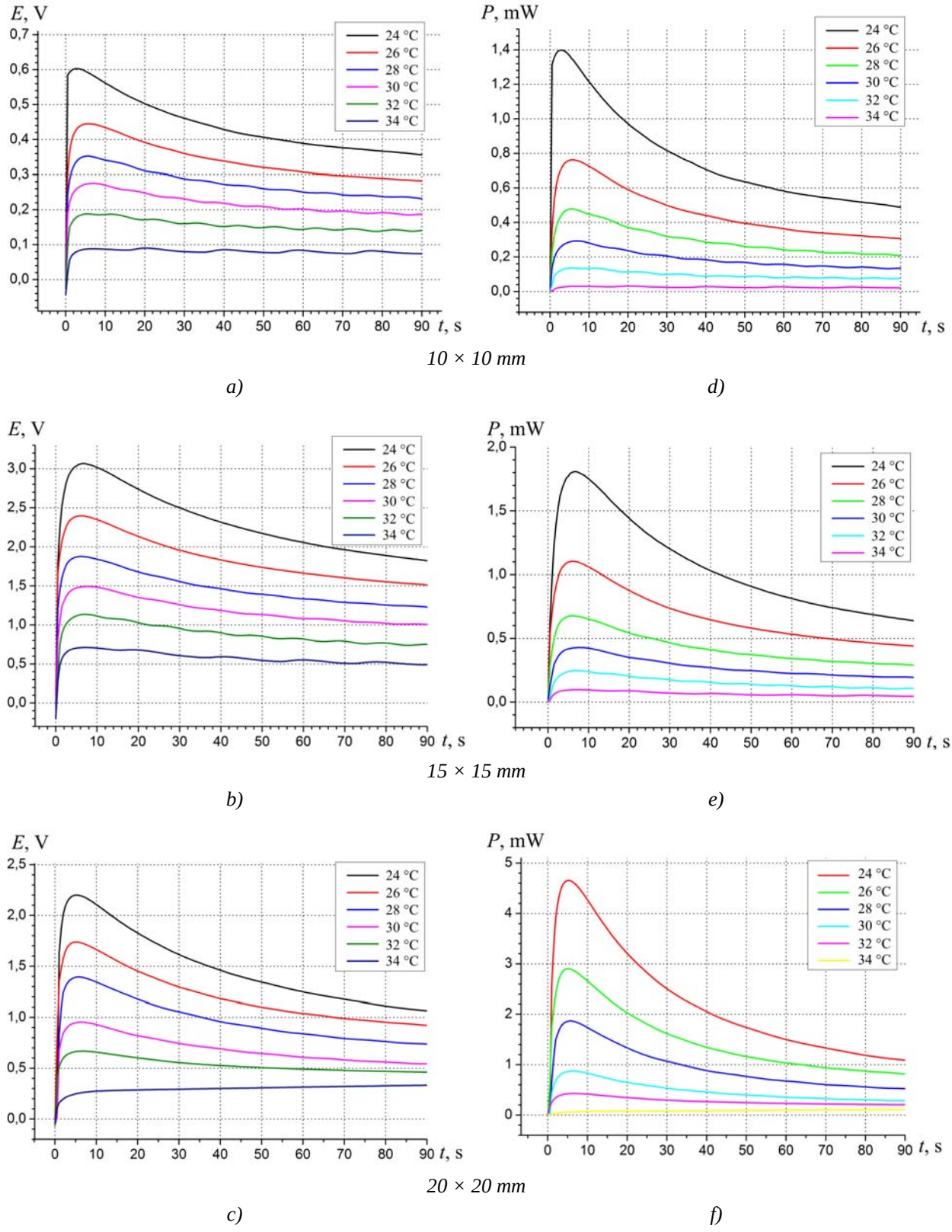

Fig. 6. Dynamics of change in the EMF (a,b, c) and electric power (d, e, f) of experimental thermoelectric microgenerators: a), d) microgenerator with dimensions 10 × 10 mm; b), e) microgenerator with dimensions 15 × 15 mm; c), f) microgenerator with dimensions 20 × 20 mm.

Apparently this peculiarity is due to imperfection of physical model, namely the absence from the side of contact between thermoelectric microgenerator and skin surface of a connecting layer which is an additional thermal capacity, resulting in reduction of thermal flux through microgenerator, hence, microgenerator characteristics. Moreover, a more real physical model should take into account a transient thermal layer between connecting plates and skin, however, to begin with, we will neglect it, since it is unkown.

Therefore, the constructed physical model should be improved through account of additional element, namely connecting layer (interlayer of POS-61 solder in the form of plates connecting thermogenerator legs) on the side of contact between thermoelectric microgenerator and skin surface.

6. Account of connecting plates and comparison of the results

Due to a divergence between the experimental data and the results of computer simulation, a physical model on the side of contact between thermoelectric microgenerator and surface skin was complemented with a continuous layer of POS-61 solder, assuring connection of legs. Following that, repated calculations of the energy characteristics of thermoelectric microgenerators were made that confirmed the assumption on the importance of this layer. A partial case of such comparison is given in Fig. 10 – 11 for a thermoelectric microgenerator with dimensions 15 × 15 mm at ambient temperature T = 24 °C.

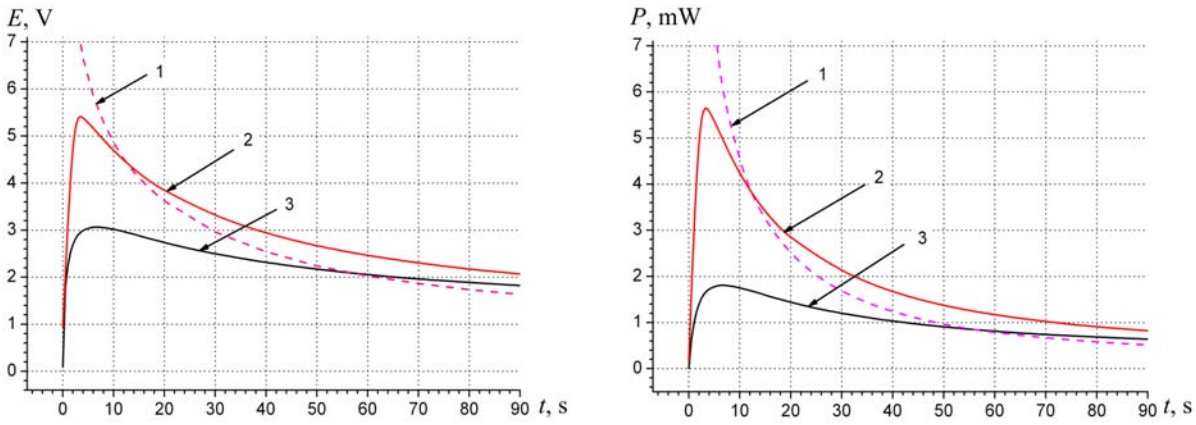

Fig. 7. Comparison of calculated and experimental results of EMF (a) and electric power (b) time dependence for a thermoelectric microgenerator with dimensions 15 × 15 mm with regard to connecting plates. (1 –computer simulation without regard to connecting layer;2 – computer simulation with regard to connecting layer; 3 – experiment).

The resulting coincidence between the experiment and computer calculations without regard in the model of a transient thermal layer between thermal generator surface and skin testifies that the effect of this layer is minor.

As is evident from Fig.7, on the calculated curve there is an optimum whose maximum value differs from the experimental data for EMF by 45 %, for electric power by 68 %. However, in this case the divergence between the calculated and experimental data remains insatisfactory, which is probably due to connecting plates geometry.

7. Account of the effect of geometry of connecting plates and comparison of the results

As is known, technology of legs connection provides for formation on the surface of thermoelectric microgenerators an array of plane-convex solder droplets with their subsequent grinding. Finally, a typical connecting plate assumes a shape that can be pretty exactly described in Fig. 8. This figure shows dimensions of connecting plates averaged from the measurements of experimental samples of thermoelectric microgenerators 1 – 3.

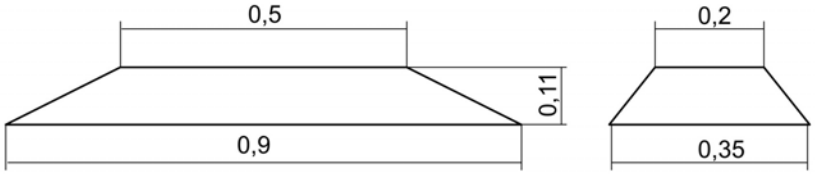

Fig. 8. Geometry of connecting plate of thermoelectric microgenerator.

With regard to geometry of connecting plates, computer simulation yielded specified energy characteristics of thermoelectric microgenerators, in particular, for a microgenerator with dimensions 15 × 15 mm (Fig. 9).

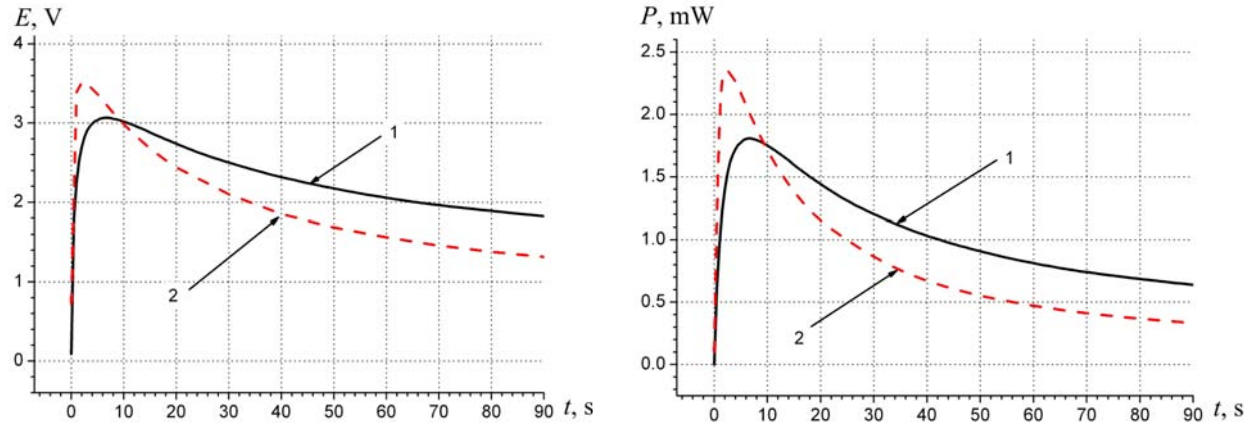

a) *b)*

Fig. 9. Comparison of calculated and experimental results of EMF (a) and electric power (b) time dependence for a thermoelectric microgenerator with dimensions 15 × 15 mm with regard to geometry of connecting plates. (1 –experiment; 2 – computer simulation with regard to geometry of connecting layer).

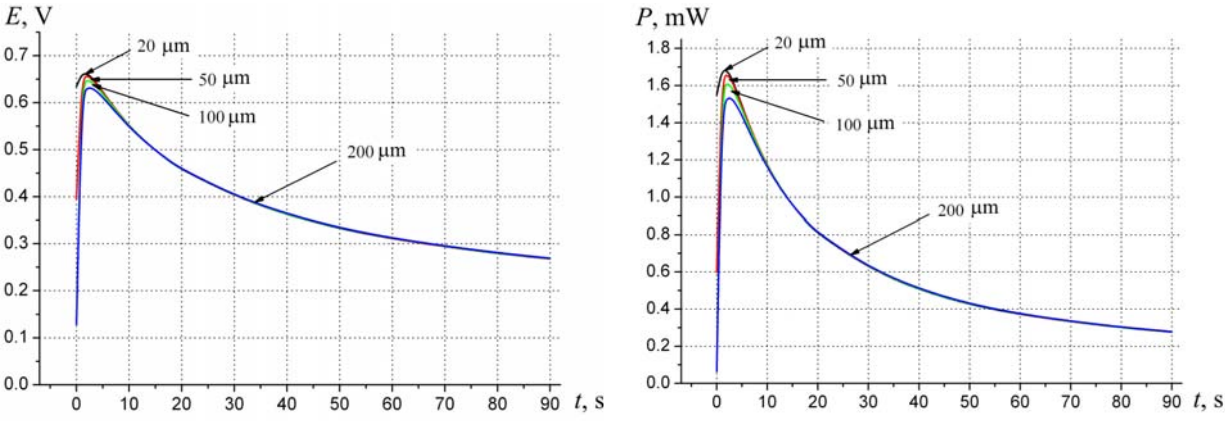

a) *b)*

Fig.10.Time dependence of EMF (a) and electric power (b) for a thermoelectric microgenerator with dimensions 10 × 10 mm for connecting plates of dissimilar thickness.

The effect of connecting plate thickness (20 μm, 50 μm, 100 μm, 200 μm) on the energy characteristics of thermoelectric microgenertaors was also investigated. As an example, Fig. 10 shows the influence of connecting plate thickness on the EMF and power of thermoelectric microgenerator with dimensions 10 × 10 mm at ambient temperature T = 24 °C.

As is evident from the plots in Fig. 10, a 10-fold change in connecting plate thickness leads to a change in EMF and electric power by 5 % and 9 %, respectively. Thus, the effect of connecting plate thickness on the energy characteristics of thermoelectric microgenerators is minor.

8. Typical time dependence of the electric energy of thermoelectric microgenerator in dynamic mode

From the curve of dynamics of electric energy storage of thermoelectric microgenerator (Fig. 11) it is seen that at the beginning of transient process the rate of electric energy storage is 2 times higher than several tens of seconds. Therefore, for a rational use of such thermoelectric microgenerator it is desirable to use special integrated electronic circuits with electric voltage stabilization and energy storage.

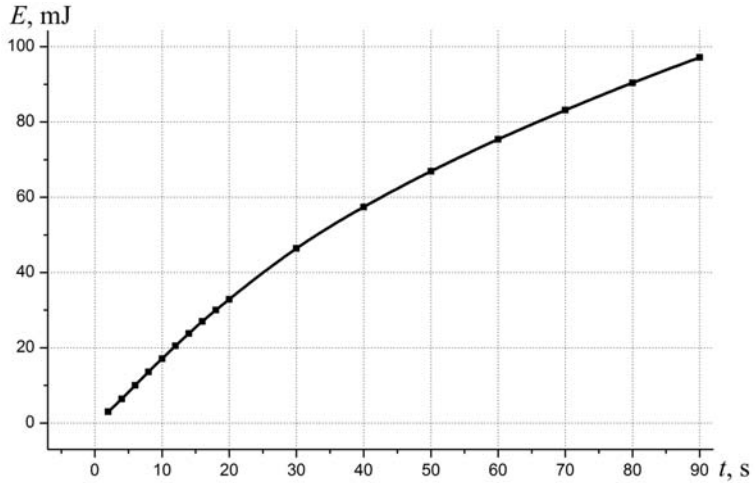

Fig. 11. Dynamics of electric energy storage of thermoelectric microgenerator with dimensions 10 × 10 mm.

9. The effect of thermoelectric microgenerator dimensions on its electric power

It is noteworthy that the work of thermoelectric microgenerator using human heat is essentially affected by its dimensions. The value of electric power is not proportional to the area of such thermal generator. With increasing area, its specific electric power is decreased. It is due to reduced effect of blood circulation bringing heat to thermal generator. Therefore, apparently it is more reasonable to use a series of thermoelectric microgenerators on given area of human body than one solid microgenerator, since in the latter case the efficiency is reduced. Moreover, arrangement of a good thermal contact is complicated. However, a study of this factor can be the subject of separate investigation.

Conclusions

1. The results of investigations confirm that when using dynamic modes at the initial steps of thermoelectric microgenerator heat-up, the released electric energy is larger than in steady-state modes. When considering a specific model it was obtained that on achieving maximum (about 5 seconds) the value of electric power is twice that in the steady-state case, which confirms the rationality of using a transient mode in short-life thermal generators.
2. In connection with a relatively low skin thermal conductivity and the fact that the experiment employed thermoelectric microgenerators where the area of connecting plates is somewhat smaller than the area of legs, the values of EMF and electric power are essentially dependent on the area of

contacting surface. Therefore, in the manufacture of such microgenerators care should be taken that the surface of contact between skin and thermal generator be maximum within each leg.

3. The resulting coincidence between the experiment and computer calculations with no account in the model of transient thermal layer between thermal generator surface and skin testifies that the effect of this layer is minor.
4. In thermoelectric microgenerators using the initial transient mode in contrast to steady-state mode it is heat sink capacity that has a dominant role in heat removal, rather than heat exchange with the environment. The latter is positive, since under such conditions one can use not heat sinks, but media with maximum possible heat capacity and thermal conductivity.

References

1. L.I. Anatychuk, *Thermoelements and Thermoelectric Devices: Handbook* (Kyiv: Naukova Dumka, 1979), 768 p.
2. L.I. Anatychuk, *Thermoelectricity, Vol. 2, Thermoelectric Power Converters* (Kyiv, Chernivtsi: Institute Thermoelectricity, 2003), 376 p.
3. L.T. Strutynska, Thermoelectric Microgenerators. State of the Art and Application Potential, *Tekhnologiya i Konstruirovaniye v Elektronnoi Apparature* **4**, 5 – 13 (2008).
4. V. Leonov and R.J.M. Vullers, Wearable Electronics Self-powered by Using Human Body Heat: The State of the Art and the Perspective, *J. Renewable and Sustainable Energy* **1**, 062701 (2009).
5. M. Lossec, B. Multon, H. Ben Ahmed, and C. Goupil, Thermoelectric Generator Placed on the Human Body: System Modeling and Energy Conversion Improvements, *Eur. Phys. J. Appl. Phys.* **52**, 11103 (2010).
6. Y. Yang, J. Liu, Evaluation of the Power-Generation Capacity of Wearable Thermoelectric Power Generator, *Front. Energy Power Eng. China* 4 (3), 346 – 357 (2010).
7. *Pat. 4106279 USA*, Wrist Watch Incorporating a Thermoelectric Generator /J. Martin and C. Piguet, 1978.
8. Pat. 6222114 USA, Portable Wrist Device/Mitamura Gen, 2001.
9. J. Paradiso, T. Starner, Human Generated Power for Mobile Electronics, *Low Power Electronics Design*, CRC Press, Fall 2004.
10. J. Paradiso, Energy Scavenging for Mobile Computing, *Responsive Environments Group. MIT Media Lab*. http://www.media.mit.edu/resenv.
11. J. Paradiso, T. Starner, Energy Scavenging for Mobile and Wireless Electronics, *IEEE CS* 5, 18 – 27 (2005).
12. G.J. Snyder, Small Thermoelectric Generators, *The Electrochemical Society Interface*, Fall 2008, p. 54 56.
13. K. Matsuzawa and M. Saka, Seiko Human Powered Quartz Watch. In *M. Rose, editor, Prospector IX: Human-Powered Systems Technologies, pages 359-384, Auburn, AL, November 1997. Space Power Institute, Auburn Univ.*
14. *Application for Utility Model* № u201315451 of 30.12.13, Pulse Meter with a Thermoelectric Power Supply /L.I.Anatychuk, R.R.Kobylianskyi, 2013.
15. *Patent of Ukraine 87400, InCl H01L 35/00,* Electronic Medical Thermometer with a Thermoelectric Power Supply / L.I. Anatychuk, R.R. Kobylianskyi, and S.B. Romanyuk, № u 2013 08794; filed 15.07.13; publ. 10.02.14, Bul. № 3.

16. L.I. Anatychuk, R.R. Kobylianskyi, On the Accuracy of Temperature Measurement by Electronic Medical Thermometer with Thermoelectric Power Supply, *J. Thermoelectricity* **5**, 75 – 79 (2013).
17. L.I. Anatychuk, R.R. Kobylianskyi, and I.A. Konstantinovich, The Effect of Thermoelectric Power Source on the Accuracy of Temperature and Heat Flux Measurement, *J. Thermoelectricity* **6**, 53 – 62 (2013).
18. L.I. Anatychuk, R.R. Kobylianskyi, and I.A. Konstantinovich, Thermoelectric Power Source for Electronic Medical Thermometer, *Tekhnologiya i Konstruirovaniye v Elektronnoi Apparature* 2 (2014).
19. Vladimir Leonov and Ruud J. M. Vullers. Wearable electronics self-powered by using human body heat: The state of the art and the perspective. // Journal Of Renewable And Sustainable Energy. - 1, 2009.
20. Julien Penders, Bert Gyselinckx, and Ruud Vullers, *Human: from Technology to Emerging Health Monitoring Concepts*, Holst Centre / IMEC-NL.
21. Vladimir Leonov, Tom Torfs, Ruud J.M. Vullers and Chris Van Hoof, Hybrid Thermoelectric-Photovoltaic Generators in Wireless Electroencephalography Diadem and Electrocardiography Shirt, *J. Electronic Materials 39* (9), 2010.
22. Vladimir Leonov and Ruud J. M. Vullers. Wearable electronics self-powered by using human body heat: The state of the art and the perspective. // Journal Of Renewable And Sustainable Energy. - 1, 2009.
23. Vladimir Vladimir Leonov, Tom Torfs, Chris Van Hoof, and Ruud J. M. Vullers, Smart Wireless Sensors Integrated in Clothing: an Electrocardiography System in a Shirt Powered Using Human Body Heat, *Sensors & Transducers Journal* **107** (8), 165 – 176 (2009).
24. Christl Lauterbach, Marc Strasser, Stefan Jung, and Werner Weber. *'Smart Clothes' Self-Powered by Body Heat, Infineon Technologies AG, Corporate Research, Emerging Technologies, Munich, Germany.* http://www.infineon.com.
25. A. Samarin, Electronics Embedded in Clothes, *Komponenty i Tekhnologii* **4**, 221 – 228 (2007).
26. A. Samarin, Electronics Embedded in Clothes – Technologies and Prospects, *Komponenty i Tekhnologii* **5**, 146 – 152 (2007).
27. S.C. Jiang, N. Ma, H.J. Li, and X.X. Zhang, Effects of Thermal Properties and Geometrical Dimensions on Skin Burn Injuries, *Burns* **28**, 713 – 717 (2002).
28. M.P. Cetingul, C. Herman, Identification of Skin Lesions from the Transient Thermal Response Using Infrared Imaging Technique, *IEEE*, 1219 – 1222 (2008).
29. M. Ciesielski, B. Mochnacki, and R. Szopa, Numerical Modeling of Biological Tissue Heating. Admissible Thermal Dose, *Scientific Research of the Institute of Mathematics and Computer Science* **1** (10), 11 – 20 (2011).
30. Florin Filipoiu, Andrei Ioan Bogdan and Iulia Maria Carstea, Computer-Aided Analysis of the Heat Transfer in Skin Tissue, *Proceedings of the 3rd WSEAS Int. Conference on Finite Differences - Finite Elements - Finite Volumes - Boundary Elements*, 2010, p. 53-59.
31. Daniela Carstea, Ion Carstea, and Iulia Maria Carstea, Interdisciplinarity in Computer-Aided Analysis of Thermal Therapies, *WSEAS Transactions on Systems and Control* **6** (4), 115-124 (2011).
32. V.A. Grigoryev, V.M.Zorin, *Heat-and-Mass Transfer. Heat Engineering Experiment: Handbook* (Moscow: Energoizdat, 1982), 512 p.
33. COMSOL Multiphysics User's Guide, COMSOLAB, 2010, 804 p.

Submitted 24.06.14